The 8th European Congress on Computational Methods in Applied Sciences and Engineering
ECCOMAS Congress 2022
5-–9 June 2022, Oslo, Norway

BAYESIAN OPTIMAL SENSOR PLACEMENT FOR VIRTUAL SENSING AND STRAIN RECONSTRUCTION

TULAY ERCAN[1], OMID SEDEHI[2], COSTAS PAPADIMITRIOU[1] AND LAMBROS S. KATAFGYIOTIS[2]

[1] Department of Mechanical Engineering, University of Thessaly
Volos, 38334, Greece
e-mails: ercan@uth.gr, costasp@uth.gr

[2] Department of Civil and Environmental Engineering
The Hong Kong University of Science and Technology
Clear Water Bay, Hong Kong SAR of China
e-mails: osedehi@connect.ust.hk, katafygiotis.lambros@gmail.com

Key words: Bayesian Inference, Kullback-Liebler Divergence, Virtual Sensing, Structural Health Monitoring, Augmented Kalman Filter

Abstract. A Bayesian optimal sensor placement (OSP) framework is presented for virtual sensing in structures using output-only vibration measurements. Particularly, this probabilistic OSP scheme aims to enhance the reconstruction of dynamical responses (e.g., accelerations, displacements, strain, stresses) for updating structural reliability and safety, as well as fatigue lifetime prognosis. The OSP framework is formulated using information theory. The information gained from a sensor configuration is defined as the Kullback-Liebler divergence (KL-div) between the prior and posterior distributions of the response quantities of interest (QoI). The Gaussian nature of the response estimate for linear models of structures is employed, and the information gain is characterized in terms of the reconstruction error covariance matrix. A Kalman-based input-state estimation technique is integrated within an existing OSP strategy, aiming to obtain estimates of response QoI and their uncertainties. The design variables include the location, type and number of sensors. Heuristic algorithms are used to solve optimization problem and provide computationally efficient solutions. The effectiveness of the method is demonstrated using an example from structural dynamics.

1 INTRODUCTION

Virtual sensing refers to techniques for reconstructing the responses at unmeasured locations and the unknown loads applied on a structure using a limited number of physical sensors. Two classes of methods for virtual sensing have been widely used. The first class refers to the modal expansion technique [1] and the second class refers to filtering techniques [2, 3, 4, 5, 6, 7]. In contrast to the modal expansion technique, filtering techniques have the advantage of reconstructing the external dynamic loads applied on the structure or reconstructing the interface dynamic loads applied on a substructure, as well as fusing multi-type physical and virtual sensors (e.g. acceleration, displacement and strain measurements and predictions).

In particular, virtual sensing of dynamic strain/stress is useful for monitoring fatigue damage accumulation [8], yielding realistic fatigue estimates consistent with existing fatigue theories and based on actual structural operating conditions. Studies of strain/stress reconstruction using modal expansion and filtering techniques cn be found in [9, 10]. Application to fatigue damage estimation using a limited number of physical displacement/strain sensors can be found in [11].

Optimal sensor placement strategies can be used to provide the most informative data collected from a sensor network for accurate response and external load reconstruction. This is achieved by minimizing an index accounting for uncertainty in the predictions or maximizing a index that accounts for the information gain. Developed methods are based on minimizing a scalar measure, such as the trace, of the steady-state reconstruction error covariance of the response [12] and/or load [13] with respect to the location of sensors. Information theoretic-based methods used to optimize the sensor configuration [14, 16, 17] for parameter estimation are also extended to handle the case of virtual sensing. In these methods, the sensor network is selected to optimize the information gained from the data. Mutual information, relative entropy and KL-div are used as measures of the information gain. OSP techniques based on information theoretic methods for virtual sensing has been proposed based on the modal expansion technique for response reconstruction [14, 18].

In this work, an OSP framework is proposed for response and load reconstruction. The method is implemented for linear systems, is based on the Augmented Kalman Filtering (AKF) technique and information theory [19], and is applicable for output-only vibration measurements. An application on a square plate structure demonstrate the effectiveness of the OSP methodology for reliable virtual sensing. A systematic study is performed in order to study the effects of measurement, model and prediction errors on the OSP design.

2 VIRTUAL SENSING USING AKF

Let $\underline{x}(t) \in R^n$ be the state vector consisting of the displacement and velocity vector of the dynamic linear finite element model of a structure (with $m = n$) or the vector of modal coordinates and its derivatives assuming that a fixed number of m modes contribute to the structural response. Formulating the governing equations of motion of the structure in state-space form and converting the continuous state space equation into the discrete state space by introducing $\underline{x}_k = \underline{x}(k\Delta t)$, where k is the time index and Δt is the discretization time interval, the following discrete state-space system is obtained

$$\underline{x}_{k+1} = A\underline{x}_k + B\underline{u}_k + \underline{w}_k \tag{1}$$

where A and B are the system matrices that depend on the mass, stiffness and damping properties of the structure, $\underline{u}_k$ is the input vector assumed to be unknown, and $\underline{w}_k \sim N(\underline{0}, Q)$ the process noise assumed to be zero-mean Gaussian, with process noise covariance $Q = \sigma_x^2 diag(Q_x) \in R^{2m\times 2m}$ selected based on the magnitude of the state vector, where σ_x controls the order of magnitude of process noise.

The observation equation is given by

$$\underline{y}_k = G(\underline{\delta})\underline{x}_k + J(\underline{\delta})\underline{u}_k + \underline{v}_k \tag{2}$$

where the matrices $\underline{G}(\delta)$ and $J(\underline{\delta})$ depend on the sensor configuration $\underline{\delta}$ indicating the type,

number and location of sensors, and the measurement error term $\underline{v}_k \sim N(\underline{0}, R)$ follows a zero-mean Gaussian distribution with measurement error covariance $R \in R^{N_0 \times N_0}$. Herein R is taken to be diagonal with the i diagonal component $R^{(ii)}$ given by $R^{(ii)} = s^2 + \sigma_e^2 Q_y^{(ii)}$ [18, 20], where $Q_y^{(ii)}$ is the square of the intensity of the QoI y_i at DOF i, s denotes the value of the measurement error that depends on the sensor accuracy and characteristics, and σ_e denote the value of model error defined as a fraction of the intensity of the measured QoI.

Let $\underline{z}_k$ be the predictions at time instant t_k of various output QoI. The prediction equation takes the form

$$\underline{z}_k = \tilde{G}\underline{x}_k + \tilde{J}\underline{u}_k + \underline{\varepsilon}_k \tag{3}$$

where the matrices $\tilde{G}$ and $\tilde{J}$ depend on the type of response QoI, and the prediction error term $\underline{\varepsilon}_k \sim N(\underline{0}, R_\varepsilon)$ follows a Gaussian distribution with prediction error covariance $R_\varepsilon = \sigma_\varepsilon^2 Q_{z_i} \in R^{n_z \times n_z}$. R_ε is also taken to be diagonal with the i diagonal component given by $R_\varepsilon^{(ii)} = \sigma_\varepsilon^2 Q_{z_i}$, where Q_{z_i} is the square of the intensity of the predicted QoI $z_i(t)$, and σ_ε is the value of model error taken as a fraction of the intensity of the predicted QoI.

Herein the AKF is used for response reconstruction for linear structural systems [2]. In AKF the time evolution of the unknown load is represented by a random walk model

$$\underline{u}_{k+1} = \underline{u}_k + \underline{\eta}_k \tag{4}$$

where $\underline{u}_k \equiv \underline{u}(k\Delta t)$ is the input force at $t_k = k\Delta t$, $\underline{\eta}_k \sim N(\underline{0}, S)$ is a zero-mean Gaussian prediction error with covariance matrix $S = \alpha^2 diag(Q_u) \in R^{n_u \times n_u}$, where Q_u is the covariance of input force vector and α defines the intensity of the fluctuations of the input as a fraction of the input intensity.

In AKF the state vector $\underline{x}_k$ is augmented to include the load vector $\underline{u}_k$. Estimates of the augmented vector and its uncertainties can then be obtained using the conventional Kalman filter (KF) equations. Starting at the time instant t_k, two steps are involved to update the estimate and its uncertainty at the next time instant $t_k + \Delta t$. The time update step that does not use the data to predict a prior estimate of the augmented state vector at $t_k + \Delta t$, and the measurement update step which uses the data to update the prediction at the time $t_k + \Delta t$. A review of this formulation is presented in the original AKF paper [2].

The time update step provides a Gaussian distribution of the prior estimate of the response QoI z_i to be reconstructed with the variance of distribution, denoted by $\Sigma_{z_i}(\underline{\delta})$, to depend on the sensor configuration vector $\underline{\delta}$, the system matrices (stiffness, mass and modal damping ratios) and the covariances of the state, measurement, model and prediction errors. The measurement update step improves on the estimate by providing a Gaussian distribution with mean that depends on the measurement at time $t_k + \Delta t$ and the covariance, denoted by $\Sigma_{z_i|D}(\underline{\delta})$, to be independent of the measurements. A solution of the nonlinear Riccatti equation is involved to find the mean and the covariance at the measurement update step and estimate the posterior covariance of the state vector and then the posterior variance $\Sigma_{z_i|D}(\underline{\delta})$ of the error of the estimate.

The optimal sensor configuration problem for virtual sensing, described in the next section, uses the prior variance $\Sigma_{z_i}(\underline{\delta})$ and the posterior variance $\Sigma_{z_i|D}(\underline{\delta})$ described in terms of the sensor configuration $\underline{\delta}$. This work also exploits the fact that the prior and posterior estimates of the state or various response QoI during the time update and measurement update steps,

respectively, follow a Gaussian distribution and that both the prior and posterior covariances are independent of the data.

3 INFORMATION GAIN

The information gained from the data depends on the sensor configuration vector $\underline{\delta}$ which includes the type, number and locations of sensors. An information theoretic measure is used in this study to evaluate the usefulness of a sensor configuration. Specifically, the KL-div [19] between the prior and posterior probability distribution of the output QoI z_i is used to measure the information gained from a sensor configuration $\underline{\delta}$ for reliably estimating a response QoI z_i given a set of data D.

Using the steady-state formulation for the error covariances and exploiting the fact that both the prior and posterior probability distributions of the estimates are Gaussian and that the covariances of these distributions are independent of the data, the KL-div, i.e., the information gain using the data from a t_k to $t_k + \Delta t$ time instances, can be written in terms of the prior and posterior covariances of the errors in the estimates as follows [18]

$$U_i(\delta) = -\left[H_{z_i|D}(\delta) - H_{z_i}(\delta)\right] = -\frac{1}{2}\ln\frac{\Sigma_{z_i|D}(\underline{\delta})}{\Sigma_{z_i}(\underline{\delta})} \tag{5}$$

where $H_{z_i}(\delta)$ and $H_{z_i|D}(\delta)$ are the information entropies corresponding to the prior and posteriron Gaussian distributions at the time update and measurement update steps of the KF formulation. At each time step, the information is gained only in the measurement update step of the KF formulation. By solving the Riccati equation, the stationary prior variance $\Sigma_{z_i}(\underline{\delta})$ can be updated, giving the stationary posterior variance $\Sigma_{z_i|D}(\underline{\delta})$.

Next the information gain is extended to account for several output QoI $\underline{z_i}$, $i = 1, \ldots, n$. The information gain for n_z QoI is defined as the average information gain, given as

$$\bar{U}(\underline{\delta}) = \frac{1}{n_z}\sum_{i=1}^{n_z} U_i(\underline{\delta}) \tag{6}$$

where it is assumed that each output QoI is equally importnat in the design of the sensor configuration. Substituting (5) into (6), the average information gain that accounts for all QoI takes the form

$$U(\underline{\delta}) = -\frac{1}{2n_z}\ln\prod_{i=1}^{n_z}\frac{\Sigma_{z_i|D}(\underline{\delta})}{\Sigma_{z_i}(\underline{\delta})} \tag{7}$$

4 OPTIMAL SENSOR PLACEMENT

The design objective is to select the sensor configuration $\underline{\delta}$ (type, location, and number of sensors) that maximizes the information contained in the data for predicting the output response QoI z_i at desirable DOF or locations $i = 1, \ldots, n_z$. The design coressponds to predictions with the least uncertainty. This is achieved by maximizing the average information gain $U(\underline{\delta})$ with respect to the design variables $\underline{\delta}$. The optimal sensor configuration is denoted by $\underline{\delta}_{opt}$. The design variabless includes the type of sensors (e.g. acceleration, displacement and strain sensor) and the location of sensors. The optimal design is repeated for a different number of sensors

ranging from 1 to N_0. It can be shown that the maximum information gain in a monotonically increasing function of the number of sensors. To find the optimal number of sensors in the sensor configuration, one monitors the information gain as additional sensors are placed in the structure and stops adding sensors when the the information gain using additional sensors is relatively small. Another way is to consider cost of sensors and instrumentation maintenance and find the optimal number of sensors that maximize the information gain and minimizes the cost of instrumentation.

Herein we are interested in maximizing the information gain for fixed number of sensors and study the variation of the information gain as a function of the number of different type of sensors placed at their optimal locations. The optimization problem is solved using discrete design variables associated with either the DOF where acceleration/displacement sensors are placed or the Gauss integration points where strain sensors are placed. Details for the implement of the discrete optimization algorithms for two types of sensors simultaneously can be found in [21]. The optimization can be performed using the heuristic algorithms [15, 16] such as the modified backward sequential sensor placement (SSP) algorithm [21] and/or genetic algorithms (GA).

5 APPLICATION

The square plate structure shown in Figure 1 is used to illustrate the effectiveness of the OSP methodology. The plate is modeled by thin-shell finite elements (FE) and is fixed at the left edge. The FE mesh consists of 400 elements and 420 nodes. The number of contributing modes is considered to be eight. The lowest modal frequency is 0.96 Hz and the eight modal frequency is 17.9 Hz. The modal damping ratios are all taken to be 0.02.

The optimal location of acceleration and strain sensors is obtained for the purpose of predicting strains at all 420 elements in the structure. The acceleration sensor are assumed to be placed at each of the 420 nodes, measuring along a direction vertical to the plate surface. The strain sensors are assumed to be placed at the midpoint of each of the 400 finite elements, measuring the normal strain along the x direction on the plate surface.

The plate is subjected to an unknown concentrated load applied at the right bottom corner. One of the tasks in this work is to investigate the effect of the values of the measurement and model/prediction error covariance matrices R and R_ε on the optimal sensor placement. For this, the quantities Q_x, $Q_y^{(ii)}$ and Q_{z_i} are selected based on a nominal broadband excitation, modeled by a Gaussian white noise sequence with standard deviation σ_{wn}. Estimates of the intensities (root mean square) of the measured and predicted QoI are obtained by solving the Liapunov equation.

The values of the model error parameter σ_e and the prediction error parameter σ_ε are taken to be $\sigma_e = \sigma_\varepsilon = 0.001$ and 0.1 corresponding to small and large model errors. The values of the measurement error parameter s corresponding to two cases of small and large measurement errors are given in Table 1 for acceleration and strain sensors. These values are selected so that the measurement error is a fraction of the the intensities of the acceleration at all measured nodes and the strains for all measured finite elements along the x direction of the plate surface, normalized by the strength σ_{wn} of the white noise. The value of the covariance $S = 1$ which corresponds to $\sigma_{wn} = 1$.

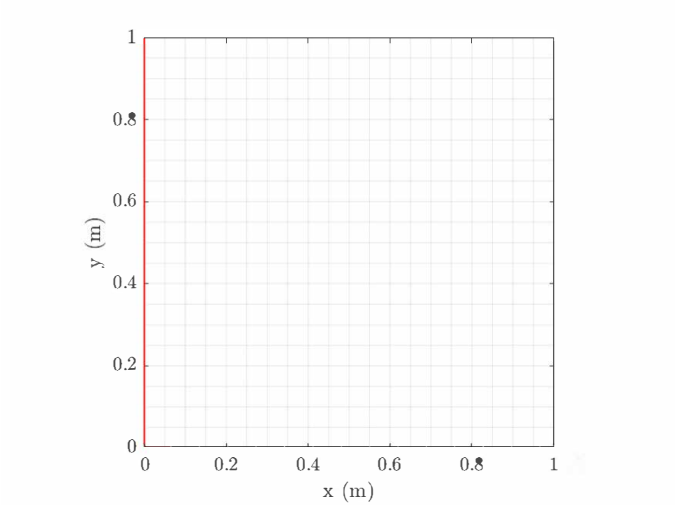

Figure 1: Square thin plate with left edge fixed (shown in red line).

Table 1: Four cases of model, measurement and prediction error, process noise, and load model error parameters. $\epsilon_{\min}$ equals to the minimum of the nodal accelerations or element strains, covering 98% of the plate surface. $\epsilon_{\max}$ and ϵ_{rms} equals respectively the maximum value and the intensity (root mean square) of the nodal acceleration or element strain in the plate surface. $\alpha = 1$ for all cases.

Cases	Error	Sensor type	$\sigma_e, \sigma_\epsilon$	s	s/ϵ_{rms}	$s/\epsilon_{\min}$	$s/\epsilon_{\max}$	σ_x
1	Small	Acceleration	10^{-3}	10^{-3}	10^{-3}	1.4×10^{-2}	2.7×10^{-4}	10^{-3}
1	Small	Strain	10^{-3}	10^{-8}	1.6×10^{-3}	10^{-2}	5.6×10^{-4}	10^{-3}
2	Large	Acceleration	10^{-1}	10^{-1}	10^{-1}	1.4×10^{0}	2.7×10^{-2}	10^{-3}
2	Large	Strain	10^{-1}	10^{-6}	1.6×10^{-1}	10^{0}	5.6×10^{-2}	10^{-3}
3	Small	Acceleration	10^{-3}	10^{-3}	10^{-3}	1.4×10^{-2}	2.7×10^{-4}	10^{-3}
3	Large	Strain	10^{-1}	10^{-6}	1.6×10^{-1}	10^{0}	5.6×10^{-2}	10^{-3}
4	Large	Acceleration	10^{-1}	10^{-1}	10^{-1}	1.4×10^{0}	2.7×10^{-2}	10^{-3}
4	Small	Strain	10^{-3}	10^{-8}	1.6×10^{-3}	10^{-2}	5.6×10^{-4}	10^{-3}

5.1 Information gain results

The information gain results as a function of the number of sensors are given in Figure 2 for up to 30 sensors for the four error cases presented in Table 1. All results are obtained using the the modified backward SSP algorithm. The first sensor is forced to be an acceleration sensor since at least one acceleration sensor is required in AKF for a stable estimation. The horizontal lines represent the maximum information $U^{all}_{\max}$ that can be reached by placing 420 acceleration and 400 strain sensors at all possible locations.

It can be seen that the information gain is an increasing function of the number of sensors placed at their optimal locations. Significant information is gained by each additional sensor for up to 9 sensors placed in the structure. For more than 9 sensors, the information gain for each additional sensor placed in the structure is relatively small (except case 4). Normalized

information gain values obtained by dividing the information gain values in Figure 2(a) by the maximum information gain value that can be achieved by placing the maximum number of 420 acceleration and 400 strain sensors are presented in Figure 2(b).

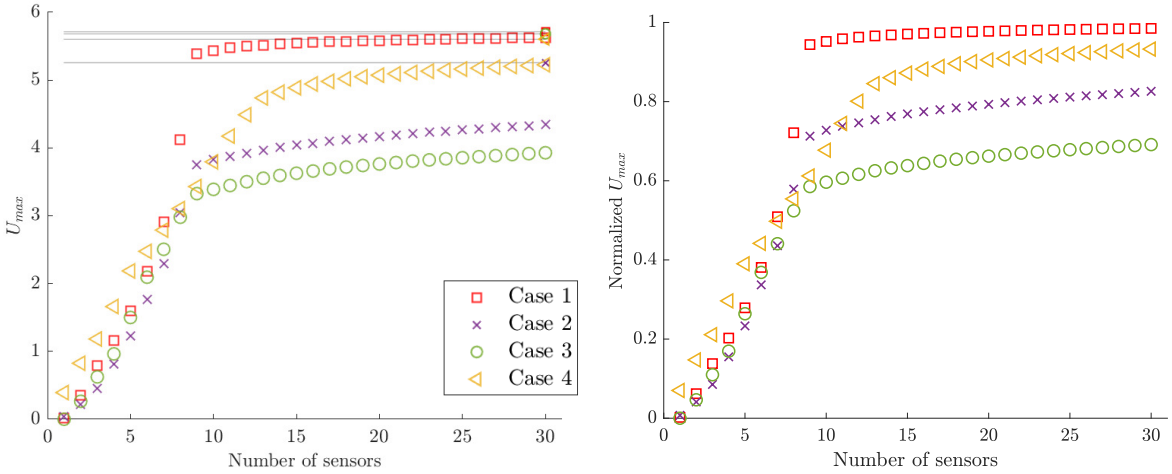

(a) **(b)**

Figure 2: Comparison of information gain results for different measurement error cases. (a) maximum information gain values, (b) normalized maximum information gain values. The maximum information gain obtained by using 820 acceleration and strain sensors (400 strain sensors and 420 acceleration sensors) placed at all possible positions, is shown with black horizontal lines.

Note that one can stop adding sensors in the structure when the information gained by each additional sensors is not significant compared to the information gained by the existing sensors. Based on the results in Figure 2, the optimal number is 9 sensors for cases 1, 2 and 3 and 13 sensors for case 4 since the increase in information gain by adding a sensor at a time is relatively small. Comparing results for error case 1 and 2, it can be observed that the information gain decreases as the measurement error or the model error increases. This means that less information is gained from noisy measurements or less accurate models which is consistent with intuition.

For the case 1 of small measurement errors for both strain and acceleration sensors, nine sensors placed at their optimal location account for 95% approximately of the maximum information $U_{\max}^{all}$. In contrast, for the case 2 of large measurement error for both strain and acceleration sensors, the information gain that can be achieved with 9 sensors placed at their optimal locations is 60% of the maximum information gain $U_{\max}^{all}$. This is due to the higher noise to signal ratio in the measurements for case 2. One can expect that more sensors are required to extract significant information. It should be noted that 30 sensors for case 2 provide only 65% of $U_{\max}^{all}$.

It is worth pointing out that in case 4 of large acceleration errors and small strain errors, the optimal number of sensors is approximately 13. Thus the number of sensors seems to depend on the level of strain and acceleration measurement errors considered. For case 3 of small

acceleration errors and large strain errors the optimal number of sensors is approximately 9, as in cases 1 and 2.

5.2 Optimal location of sensors

Figure 3(a) shows the best acceleration (circle) and strain (square) sensor locations for 9 sensors for error cases 1 and 2. The best type of sensors to be used for case 1 are 5 acceleration sensors and 4 strain sensors out of the total of 9 sensors. The 4 strain sensors are distributed on the plate far from the right edge which has a very small strain intensity and so relatively large noise-to-signal ratio. The acceleration sensors are also well distributed and placed closer to the right edge, avoiding locations closer to the fixed support, since there again the noise-to-signal ratio is expected to be smaller than the locations close to the fixed support.

Figure 3(b) shows similar results for 9 sensors for error cases 3 and 4. For case 4 there are only two acceleration sensors and 7 strain sensors in the optimal configuration due to the fact that the error in acceleration measurement is large and thus such sensors are not preferred. However, the same result is obtained for the case 3 which signifies that large errors in the strain measurements do not affect significantly the type of sensors selected. More strain sensors are preferred despite the large errors in strain measurements compared to the errors in acceleration measurements.

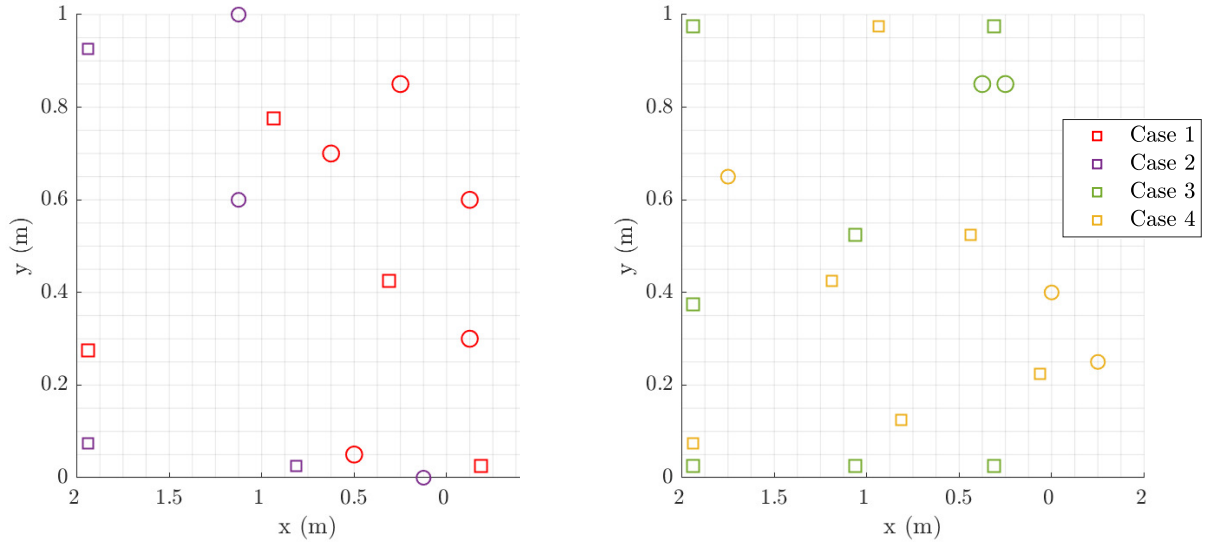

(a) **(b)**

Figure 3: Comparison of best sensor locations for 9 sensors for different measurement error cases. Acceleration and strain sensors are shown with circle and square, respectively. (a) Cases 1 and 2, (b) Cases 3 and 4.

From the results presented, it can be observed that a combination of the two type of sensors is needed to provide an effective sensor configuration. The location and the type of sensors depend on the level of model and measurement errors considered. It should be noted that the

worst sensors are found to be acceleration sensors (not shown in the figures) for all error cases, placed at the nodes closest to the left support.

6 CONCLUSIONS

The proposed optimal sensor placement methodology is based on AKF for virtual sensing and input/response reconstruction. It is applicable to linear systems or linear subcomponents of systems. It can be used to obtain the maximum information gain from an optimally design sensor configuration. The methodology can fuse different types of acceleration, displacement and strain sensors. Despite the fact that the predictions are strains, the type of sensors that are promoted for monitoring are both acceleration and strain sensors. In contrast, the optimal sensor placement based on modal expansion [18] limits the type of sensors that can be used. To implement the methodology one has to decide of the levels of the errors, such as process noise, measurement, model and prediction errors, since these errors are found to affect the information gain and the optimal sensor configuration. The higher the measurement and model error the less the information gained from the optimal sensor configuration. It is also found that a small number of sensors of the order of the number of contributing modes yields the most information. Adding more sensors the information increase is not significant for small measurement error. For large measurement error such increase can be significant but the information gain is incremental, requiring a lot of sensors to get to the maximum information. Although the methodology is demonstrated for response predictions, it can readily be used for input reconstruction as well. The proposed OSP framework was used to select the optimal number of acceleration and strain sensors. However, it can readily be applied to optimize the location of an available fixed number of strain and acceleration sensors.

The reconstructed responses and inputs provided by the proposed OSP methodology are important for providing more accurate data-driven safety estimates of systems. Reconstructing stress response time histories, in particular, are useful for reliably predicting fatigue damage accumulation estimates.

ACKNOWLEDGEMENT

This project has received funding from the European Union's Horizon 2020 research and innovation programme under the Marie Skłodowska-Curie grant agreement No 764547.

REFERENCES

[1] Kullaa, J. Bayesian virtual sensing in structural dynamics. *Mechanical Systems and Signal Processing*. (2019) **115**:497-513.

[2] Lourens, E., Reynders, E., De Roeck, G., Degrande, G. and Lombaert, G. An augmented Kalman filter for force identification in structural dynamics. *Mechanical Systems and Signal Processing*. (2012) **27**:446-460.

[3] Lourens, E., Papadimitriou, C., Gillijns, S., Reynders, E., De Roeck, G. and Lombaert, G. Joint input-response estimation for structural systems based on reduced-order models and vibration data from a limited number of sensors. *Mechanical Systems and Signal Processing*. (2012) **29**:310-327.

[4] Eftekhar Azam, S., Chatzi, E. and Papadimitriou, C. A dual Kalman filter approach for state estimation via output-only acceleration measurements. *Mechanical Systems and Signal Processing*. (2015) **60**:866-886.

[5] Naets, F., Cuadrado, J. and Desmet, W. Stable force identification in structural dynamics using Kalman filtering and dummy-measurements. *Mechanical Systems and Signal Processing*. (2015) **50-51**:235-248.

[6] Dertimanis, V., Chatzi, E., Azam, S. and Papadimitriou, C. Input-state-parameter estimation of structural systems from limited output information. *Mechanical Systems and Signal Processing*. (2019) **126**:711-746.

[7] Impraimakis, M. and Smyth, A. An unscented Kalman filter method for real time input-parameter-state estimation. *Mechanical Systems And Signal Processing*. (2022) **162**, 108026.

[8] Papadimitriou, C., Fritzen, C., Kraemer, P. and Ntotsios, E. Fatigue predictions in entire body of metallic structures from a limited number of vibration sensors using Kalman filtering. *Structural Control and Health Monitoring*. (2011) **18**:554-573.

[9] Maes, K., Iliopoulos, A., Weijtjens, W., Devriendt, C. and Lombaert, G. Dynamic strain estimation for fatigue assessment of an offshore monopile wind turbine using filtering and modal expansion algorithms. *Mechanical Systems and Signal Processing*. (2016) **76**:592-611.

[10] Vettori, S., Lorenzo, E., Cumbo, R., Musella, U., Tamarozzi, T., Peeters, B. and Chatzi, E. Kalman-Based virtual sensing for improvement of service response replication in environmental tests. *Model Validation and Uncertainty Quantification, Vol. 3*. (2020) 93-106.

[11] Maes, K. and Lombaert, G. Fatigue monitoring of railway bridges by means of virtual sensing. *Proceedings of The Belgian and Dutch National Groups of IABSE - Young Engineers Colloquium 2019,YEC2019*. (2019) 24-25.

[12] Hernandez, E. Efficient sensor placement for state estimation in structural dynamics. *Mechanical Systems and Signal Processing*. **85**:(2017) 789-800.

[13] Cumbo, R., Mazzanti, L., Tamarozzi, T., Jiranek, P., Desmet, W. and Naets, F. Advanced optimal sensor placement for Kalman-based multiple-input estimation. *Mechanical Systems and Signal Processing*. (2021) **160**, 107830.

[14] Papadimitriou, C., Haralampidis, Y. and Sobczyk, K. Optimal experimental design in stochastic structural dynamics. *Probabilistic Engineering Mechanics*. (2005) **20**:67-78.

[15] Papadimitriou, C. Optimal sensor placement methodology for parametric identification of structural systems. *Journal of Sound and Vibration*. (2004) **278**:923-947.

[16] Bhattacharyya, P. and Beck, J. Exploiting convexification for Bayesian optimal sensor placement by maximization of mutual information. *Structural Control and Health Monitoring*. (2020) **27**:1-18.

[17] Ebrahimian, H., Astroza, R., Conte, J. and Bitmead, R. Information-theoretic approach for identifiability assessment of nonlinear structural finite-element models. *Journal of Engineering Mechanics*. (2019) **145**, 04019039.

[18] Ercan, T. and Papadimitriou, C. Optimal sensor placement for reliable virtual sensing using modal expansion and information theory. *Sensors*. (2021) **21**, 3400.

[19] Kullback, S. and Leibler, R. On information and sufficiency. *The Annals of Mathematical Statistics*. (1951) **22**:79-86.

[20] Papadimitriou, C. and Lombaert, G. The effect of prediction error correlation on optimal sensor placement in structural dynamics. *Mechanical Systems and Signal Processing*. (2012) **28**:105-127.

[21] Ercan, T. and Sedehi, O. and Katafygiotis, L. S. and Papadimitriou, C. Information theoretic-based optimal sensor placement for virtual sensing using augmented Kalman filtering. Submitted to MSSP. (2022) doi = 10.5281/zenodo.6508382.